ELSEVIER

Separation and Purification Technology 32 (2003) 255–264

Separation and Purification Technology

www.elsevier.com/locate/seppur

Performance of hydrophobic and hydrophilic silica membrane reactors for the water gas shift reaction

Sabine Giessler, Luke Jordan, João C. Diniz da Costa *, G.Q. (Max) Lu

Nanomaterials Centre and Department of Chemical Engineering, The University of Queensland, Brisbane 4072, Qld., Australia

Abstract

In this study, a novel molecular sieve silica (MSS) membrane packed bed reactor (PBR) using a $Cu/ZnO/Al_2O_3$ catalyst was applied to the low-temperature water gas shift reaction (WGS). Best permeation results were H_2 permeances of 1.5×10^{-6} mol s^{-1} m^{-2} Pa^{-1}, H_2/CO_2 selectivities of 8 and H_2/N_2 selectivities of 18. It was shown that an operation with a sweep gas flow of 80 cm^3 min^{-1}, a feed flow rate of 50 cm^3 min^{-1} and a H_2O/CO molar ratio of one at 280 °C reached a 99% CO conversion. This is well above the thermodynamic equilibrium and achievable PBR conversion. Hydrophilic membranes underwent pore widening during the reaction while hydrophobic membranes indicated no such behaviour and also showed increased H_2 permeation with temperature, a characteristic of activated transport.

Keywords: Hydrophilic and hydrophobic membranes; Molecular sieve silica (MSS); Packed bed membrane reactor (PBMR); Water gas shift (WGS) reaction; CO conversion

1. Introduction

The water gas shift (WGS) reaction is an important reaction in processes where carbon monoxide together with steam is converted to carbon dioxide and hydrogen. The reaction is exothermic and thermodynamically favoured at lower temperatures in the region of 180–250 °C mainly using copper-based catalysts [1–4]. The idea of using membrane reactors for WGS reaction is not new, but novel molecular sieve silica (MSS) membranes are becoming very competitive against traditional non-hydrostable metal membranes (e.g. palladium and its alloys). Economic factors also play an important role for membrane reactor application, in particular driven by the enormous payoff envisaged for fulfilling the continuously increasing H_2 demand in the refinery industry and for fuel cell technology.

The hydrothermal stability of MSS membranes is an area of increasing research interest, in particular applications such as membrane reactors and gas separation of process streams containing hot steam [5]. Various research groups have produced high quality silica derived membranes [6–10] with pore sizes with molecular dimensions in the region of 3–4 Å. These membranes are ideal for gas separation, but contain a large amount of

* Corresponding author. Tel.: +61-7-3365-6960; fax: +61-7-3365-4199.

E-mail address: joedac@cheque.uq.edu.au (J.C. Diniz da Costa).

1383-5866/03/$ - see front matter
doi:10.1016/S1383-5866(03)00069-8

Nomenclature

IGCC	integrated coal gasification combined cycles
MTES	methyltriethoxysilane
MSS	molecular sieve silica
TEOS	tetraethylorthosilicate
PBR	packed bed reactor
PBMR	membrane packed bed reactor
PSD	pore size distribution
P	permeance (mol m^{-2} s^{-1} Pa^{-1})
R	molar ratio of H_2O/CO (−)
S	selectivity factor (−)
WGS	water gas shift

silanol groups which are hydrophilic and easily react with water molecules, thus resulting in further changes in the matrix of silica-derived materials.

Novel synthesis methods designed to increase the hydrophobicity of MSS membranes include thermal treatment or surface modification using template agents. Templates can be classified as organic covalent ligands (such as methyl groups [11]) or non-covalently bonded (such as surfactants [12]). De Vos et al. [11] recently embedded methyltriethoxysilane (MTES) into a sol–gel process involving the reaction of tetraethylorthosilicate (TEOS), water, ethanol and acid. This process introduces methyl groups to the silica matrix to enhance hydrophobicity. These membranes showed good permeances while selectivities decreased due to a broader pore size distribution (PSD) in comparison to membranes prepared without MTES. Various research groups have used non-covalently bonded organic templates, such as C6 and C16 surfactants [10] and alkyltriethoxysilanes [12], to tailor the pore size of intermediate or top layers of membranes.

In this study, we test novel hydrophobic and conventional standard hydrophilic MSS membranes as part of a membrane reactor system for the H_2 production in the low-temperature WGS reaction. The membrane reactor used in this work is a flat membrane module with a ternary Cu-based catalyst bed. The influence of the membrane characteristics on the reactor performance in terms of their hydrophobicity, selectivity and permeability is investigated. The characteristics of the membranes for transport and selectivity stability are tested in gas permeation experiments before and after their usage in the membrane reactor. Catalyst activity testing is carried out with the Cu/ZnO/Al_2O_3 catalyst placed in a hollow quartz tube similar to a packed bed reactor (PBR). The CO conversion is studied by correlating it to the feed flow rate and temperature. The operating conditions of the packed bed membrane reactor (PBMR) are optimised for CO conversion by adjusting the H_2O/CO molar ratio (R), the temperature, the gas feed flow and composition. The influence of the nitrogen sweep gas in the permeate side is also investigated in the context of optimising parameters.

2. Materials and experimental

2.1. Membrane preparation

The support platelets used for the membranes were α-alumina (99.8% purity) with an average pore size of 0.5–1.0 μm and a porosity of 30%. The supports were first smoothed with sandpaper 600 and 1200 grades and then calcined at 1 °C min^{-1} up to 600 °C with a holding period of 4 h. The calcination of the supports was carried out to avoid heat stresses of subsequent film layers during calcination which may render ineffective films with micro-cracks. The supports were then coated twice with Locron alumina (supplied by

Bayer), hereinafter called sol L, and calcined at the same conditions as the α-alumina supports. Subsequent intermediate and top layers were silica derived as described elsewhere [13,11] and based on a two-step catalysed hydrolysis sol–gel process. TEOS and MTES were employed as the silica precursors mixed with ethanol (EtOH), nitric acid (HNO_3) and distilled water.

The sol–gel compositions developed in this work and respective sample notations are listed in Table 1. In the case of solutions S1 and S2, an additional 4.2 wt.% of C6-surfactant (triethylhexylammonium bromide) was mixed into the final solution at ambient temperature [10]. Prior to dip-coating the supports, the sols are diluted with ethanol 1:2 for the intermediate layer and 1:19 for the top layer. The intermediate and top layers were calcined with heating rates 1 and 0.5 °C min^{-1} up to 500 °C with a holding period of 4 h. The final membrane thickness (intermediate and top film layers) was in the order of 250–300 nm. Table 2 lists the characteristics of the hydrophobic (M1) and hydrophilic (M2) membranes synthesised for this study, including H_2 permeation, H_2/CO_2 and H_2/N_2 permselectivity results.

2.2. Catalyst preparation

Although binary and ternary copper-based catalysts are commercially available, in this research a $Cu/ZnO/Al_2O_3$ catalyst was prepared by co-precipitation. In this system, zinc oxide is used as a structural stabiliser and promoter whereas aluminium oxide is used to improve the catalyst dispersion. For every 10 g of the final catalyst, we used 17.3 g of $Zn(NO_3)_2 \cdot 6H_2O$, 10 g of $Cu(NO_3)_2 \cdot 3H_2O$ and 14.7 g of $Al(NO_3)_3 \cdot 9H_2O$ which were dissolved in water (200 ml, 70 °C) and then mixed with sodium carbonate solution (25 g in 100 ml). After 1.5 h precipitation, the solution was filtered, washed with water and dried. The collected precipitate was calcined to form oxides at 500 °C with a heating rate of 2 °C min^{-1}, and a holding time of 3 h. The catalyst weight percent composition was $Cu(33)/ZnO(47)/Al_2O_3(20)$ with a density of 414.6 kg m^{-3}.

2.3. Gas permeation, membrane reactor and catalyst activity tests

Membrane gas permeation was measured using a dead-end mode for single gas permeation. The permeation rig consisted of two MKS-1 pressure transducers, a membrane module, a permeate reservoir, a vacuum pump and a computer to log the data from the pressure transducers. In the dead end mode, the permeate reservoir pressure changed from an initial vacuum to a final transient condition [22]. The permeation rates of hydrogen, carbon dioxide and nitrogen were measured at temperatures ranging from ambient to 200 °C with a pressure difference of 1 bar across the membrane.

The activity tests of the catalyst were performed in a PBR with 180 mg catalyst powder (≈ 100 μm size) loaded on a quartz frit in the middle of a flow quartz-tube reactor (12 mm ID). The system was heated in an electric furnace (temperatures between 150 and 450 °C). All reaction experiments were carried out at atmospheric pressure and feed flows between 50 and 400 cm^3 min^{-1}. The feed flow contained steam and CO in a molar ratio varying between 0.6 and 2.5.

The steam was produced by injecting water into the gas stream using a calibrated water pump. The steam was vaporised and entered the membrane

Table 1
Molar composition of the used sols

ID	TEOS	MTES	EtOH	HNO_3	H_2O	C6-surfactant (wt.%)
S1	1	1	7.6	0.004	5.0	4.2
S2	1	0	3.8	0.004	5.0	4.2
S3	0.9	0.1	3.8	0.056	5.0	–
S4	1	0	3.8	0.004	5.0	–

Table 2
Characteristics of applied membranes M1–M6

ID	Number of layers	Surface structure	H_2 permeance (200 °C) $\times 10^{-7}$ (mol s^{-1} m^{-2} Pa^{-1})	H_2/CO_2 (200 °C)	H_2/N_2 (100 °C)
M1	2L+2S1+2S2	Hydrophobic	15	6	8
M2	2L+2S3+4S4 JMS	Hydrophilic	0.07	11	18

reactor via a heated gas feed line in order to avoid water condensation. The gas sample concentrations were measured for H_2, CO_2 and CO using a Shimadzu GC 17A (TCD detector) fitted with a PorapakQ column. Helium was employed as the sweeping gas. To facilitate the collection of gas samples for the GC analysis, a condenser was installed at the reactor exit to remove water from the gas stream.

The membrane reactor performance was measured using the test system shown in Fig. 1. The permeate side was open to the atmosphere. The membrane has a flat-sheet configuration, which is not optimal for a membrane reactor, but it can be used to study the concept and feasibility of employing MSS membranes in a reactor [14]. The membrane reactor consisted of the membrane fixed between two coupling pieces (feed and permeate side). In order to achieve an even distribution of the feed over the bed, glass wool was filled into the feed line. The feed flows varied between 50 and 400 cm^3 min^{-1}, with H_2O/CO molar ratios of 0.6–2.5. The permeate coupling piece contained a line for the sweep gas which was N_2 in the flow range of 0–300 cm^3 min^{-1}. On the top side of the membrane a graphite gasket was fitted into which 180 mg of catalyst was filled. Silicon O-rings were employed for sealing the module, making operation possible at up to 330 °C. The temperature was controlled with a

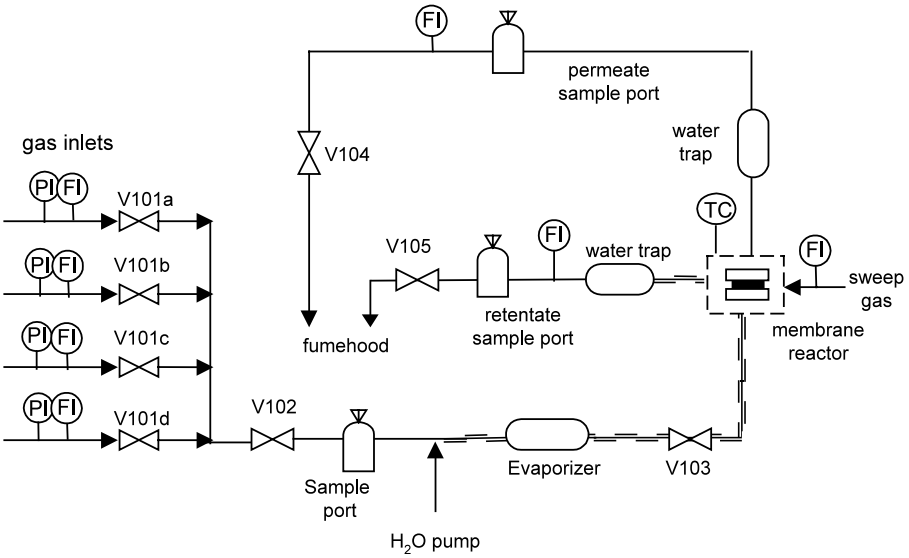

Fig. 1. Schematic system for the membrane reactor.

PID controller in the range 150–330 °C. Gas samples were taken from the sample ports in the feed, the retentate and the permeate lines.

3. Results and discussion

3.1. Gas permeation results

Representative results for permeation tests and H_2/CO_2 permselectivity for the hydrophobic membranes (M1), and for the hydrophilic membranes (M2) are depicted in Figs. 2 and 3, respectively. It is observed that H_2 permeance generally tended to increase with temperature, a characteristic of activated transport. These results indicated that these membranes were of a high quality and had a very narrow PSD, small enough to allow the permeation of a large quantity of the smaller molecules (H_2) while having a reduced capacity for the large molecule (CO_2) to diffuse through the membrane. This is in line with work reported in the literature [11,15] suggesting that pore size exclusion was a major separation mechanism for high quality MSS membranes activated by temperature. On the other hand, CO_2 permeation showed an opposite behaviour to H_2 permeation, as it decreased with temperature. As reported by de Vos et al. [8], this behaviour occurs to MSS membranes, given that the activation energy for CO_2 has been shown to assume slight negative values at low temperatures.

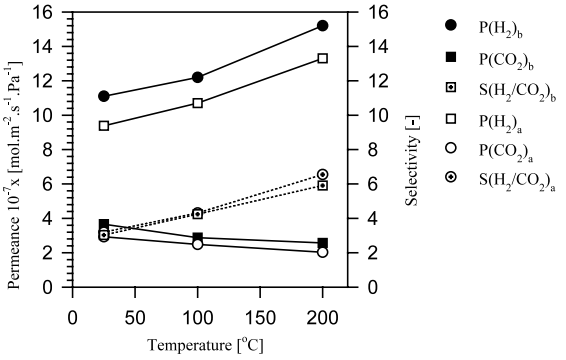

Fig. 2. Temperature dependence performance of the hydrophobic membrane (M1) shown as $(\text{before})_b$ and $(\text{after})_a$ use in PBMR.

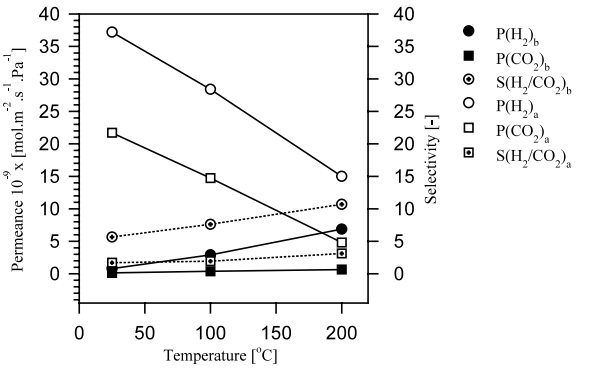

Fig. 3. Temperature dependence performance of the hydrophilic membrane (M2) shown as $(\text{before})_b$ and $(\text{after})_a$ use in PBMR.

Having said that, there were differences for the permeation regimes before and after use in the membrane reactor. The hydrophobic membrane (M1) performed reasonably well although a reduction in permeance of 10–15% (H_2) and of 10–20% (CO_2).was observed These changes had, however, very little impact upon the H_2/CO_2 permselectivity. On the other hand, Fig. 3 revealed much more significant changes in the gas permeation properties of the hydrophilic membrane (M2). H_2 and CO_2 permeances increased one and two orders of magnitude after use in the reactor, respectively, whilst permselectivity decreased approximately 5-fold. Furthermore, H_2 permeation no longer appeared to be an activated transport because permeance decreased with temperature.

These results strongly suggested that the water vapour induced structural changes to the membrane film, in particular with the hydrophilic membrane where changes in permeation and permselectivity were quite accentuated. As the permeation regime changed from activated to non-activated transport, coupled with an increase in permeation, there was an indication that the membrane undergoes pore enlargement after use in the membrane reactor. As the PSD broadened, large pores ($dp > 10$ Å) caused parallel flux, which complies with Knudsen or Pouseille mass flow mechanisms. Such a fate was not at all met by the hydrophobic membrane, which showed a small reduction in permeation. The performance of the hydrophobic membranes suggested that a slight

pore closure has occurred, in particular that the permselectivity was basically kept similar to both situations e.g. before and after the use in the membrane reactor system. The influence of water vapour on the pore structure and PSD of the formed xerogels are discussed in more detail by Giessler et al. [5,16].

The H_2 permeation of the membranes tested was one order of magnitude below the results for hydrophilic MSS membranes reported in the literature [8,10]. Nevertheless, the permeation results for hydrophobic membranes are similar to those reported recently by de Vos et al. [11]. In addition, the performance of the membranes produced in this work fit easily into the permeation/selectivity range given for H_2 selective microporous membranes by Prabhu et al. [17]. Although great care was taken during the synthesis of the membranes, this process was carried out in normal laboratory conditions, which presented a reasonably high possibility of film defect due to dust. One way of addressing this problem is by constructing more layers of silica film resulting in thickness increase. In this work, at least six layers were coated and resulting in a film thickness in the region of one order of magnitude thicker than those produced in clean rooms by de Vos et al. [11] and Tsai et al. [10]. As the flux is inversely proportional to the thickness of membranes, the permeation results in this study are deemed to be lower than those reported in the literature.

3.2. Temperature dependence of the CO conversion

In Fig. 4, the effect of temperature on the CO conversion in the membrane reactor and the PBR demonstrated that the maximum experimental conversions attained were at a temperature of 280 °C. The membrane reactor resulted in a higher CO conversion of 93%, while the PBR achieved a maximum of 84%. Fig. 4 also showed that the drop in CO conversion observed for the hydrophobic membrane (M1) at the elevated temperatures was reasonably steady as expected due to a steady decline in catalyst activity (see PBR shape). In contrast, significant drop in CO conversion was obtained for the hydrophilic membrane (M2) at temperatures above 300 °C, especially at a higher feed flow rate of 80 $cm^3 min^{-1}$. This was likely to be the result of membrane structural degradation as discussed above.

As the equilibrium conversion was achieved and surpassed at 280 °C, the use of membrane reactors became extremely advantageous as the membrane life is enhanced while leading to cost and energy consumption reductions, mainly attributed to lower reaction temperatures. The reason for the better performance was the withdrawal of one of the products, namely H_2, which shifted the chemical equilibrium resulting in higher conversions.

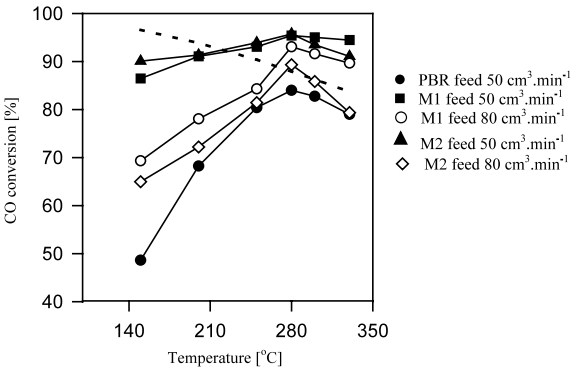

Fig. 4. Temperature dependence of CO conversion for the PBMR and PBR ($R = 1.0$, no sweep gas).

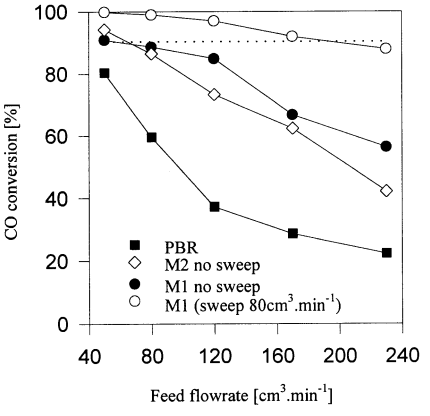

Fig. 5. Dependence of CO conversion on the feed flow rate ($R = 1$, $T = 250$ °C).

3.3. Dependence of CO conversion on the total feed flow rate

The CO conversion dependence on the total volumetric feed flow rate is shown in Fig. 5. The results were generated for both the membrane reactor and the PBR at a temperature of 250 °C and a H_2O/CO molar feed ratio of one. It is observed that CO conversion decreased with increasing feed flow rate in all cases, in particular for the hydrophilic membrane (M2). The CO conversion for the hydrophobic membrane (M1) stayed above the equilibrium conversion for a sweep gas flow of 80 $cm^3\ min^{-1}$ as long as the feed flow was smaller than 200 $cm^3\ min^{-1}$.

The highest CO conversion achieved was at 50 $cm^3\ min^{-1}$ for both PBR and PBMR with or without sweep gas. Qualitatively, this behaviour was similar to that reported by Basile et al. [5] for a membrane reactor incorporating a composite palladium dense membrane. Fig. 5 showed that the CO conversion decreased for the PBR of almost 60% when the feed flow rate was increased from 50 to 230 $cm^3\ min^{-1}$. The loss in CO conversion in the same feed range for the hydrophobic membrane (M1) was only 30%, whereas the hydrophilic membrane (M2) showed a loss of 50%. Hence, PBMRs (i.e. containing the membrane reactor) significantly outperformed the PBR system. The hydrophobic membrane (M1) also performed better than the hydrophilic one (M2), except that the CO conversion of the latter was only marginally better for the condition of without sweep gas at the lower feed flow rate of 50 $cm^3\ min^{-1}$.

3.4. Influence of nitrogen sweep gas in the permeate line of the PBMR on the conversion

Fig. 6 depicts the results from varying the nitrogen sweep gas in the permeate line at a temperature of 250 °C, R equals to one and a feed flow of 50 $cm^3\ min^{-1}$. The sweep gas influenced upon the nature of the membrane in use, as the CO conversion varied above the equilibrium conversion, but was generally higher for the hydrophobic membrane than the hydrophilic one. These experiments resulted in the best

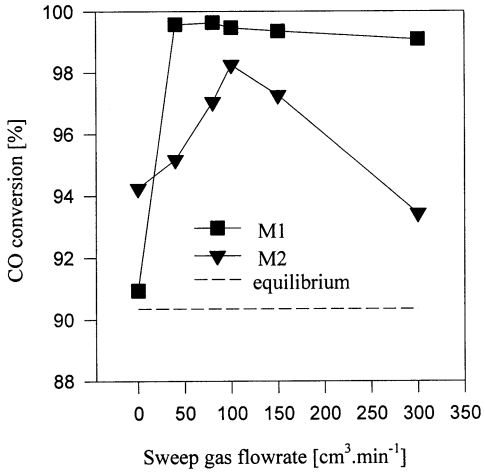

Fig. 6. Effect of sweep gas flow rate on CO conversion (feed flow 50 $cm^3\ min^{-1}$, $T = 250$ °C, $R = 1$).

CO conversion of 99% for a sweep flow rate of 80 $cm^3\ min^{-1}$ which are in the range of those reported by Armor [18].

One of the most distinct relationships for CO conversion and sweep gas flow rate for different membranes was observed at high sweep gas flow rates. The hydrophobic membrane (M1) showed a significant increase in CO conversion upon the addition of sweep gas to a flow rate of 40 $cm^3\ min^{-1}$, with the high conversions being sustained with further increases in sweep gas flow rates up to 300 $cm^3\ min^{-1}$. Basile et al. [19] reported similar trends for their composite palladium membranes. Conversely, the hydrophilic membrane (M2) presented a lower rise in CO conversion with the introduction of sweep gas. An optimum conversion (below that achieved for membrane M1) was reached at a sweep gas flow rate of 100 $cm^3\ min^{-1}$, before rapidly declining at flow rates higher than 150 $cm^3\ min^{-1}$. This behaviour is also observed by varying the feed flow rates to 70 and 100 $cm^3\ min^{-1}$ as seen in Fig. 7. Although this trend was exhibited for mesoporous membranes used by Criscuoli et al. [20], it would not be expected that the same occurs for microporous MSS membranes being used in this research. However, as degradation in the membrane microstructure occurred as discussed above and showed in Fig. 3, the results

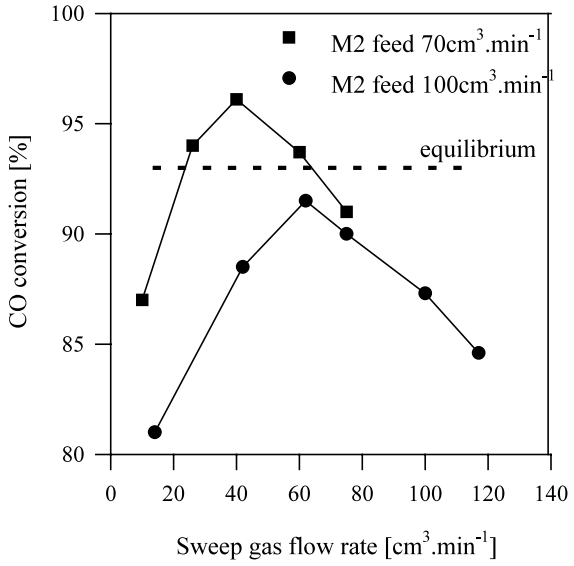

Fig. 7. Effect of sweep gas flow rate on CO conversion ($T = 200$ °C, $R = 1$).

for hydrophilic membranes are in line with those reported for mesoporous membranes.

In Fig. 7, the feed flow rate of 70 $cm^3\ min^{-1}$ resulted in CO conversion above equilibrium conversion for sweep gas flow rates between 20 and 60 $cm^3\ min^{-1}$. The best CO conversion was reached at a sweep gas rate of 40 $cm^3\ min^{-1}$. The same experiment carried out at a feed flow rate of 100 $cm^3\ min^{-1}$ did not surpass the equilibrium value (94%) while the highest CO conversion of 91% for this test was observed at a sweep flow rate of 60 $cm^3\ min^{-1}$. These results suggest that the sweep gas flow rate should be operated at about half of the feed flow rate to achieve best CO conversions in the case of the hydrophilic membranes. By the same token, hydrophobic membranes performed quite comfortably for sweep gas flow rate varying from half to about the same as the feed flow rate (see Fig. 6).

3.5. Influence of the molar feed ratio on the CO conversion

Fig. 8 shows the relationship between CO conversion and the H_2O/CO molar ratio in the feed stream. The feed flow rate was set at 50 $cm^3\ min^{-1}$ at 250 °C. Important observations included that equilibrium conversions are surpassed for H_2O/CO $R < 1$ for both membranes. The maximum increase in CO conversion with respect to the equilibrium values occurred in the range of 0.9–1.0. The CO conversions for the PBR was always slightly below the equilibrium conversions.

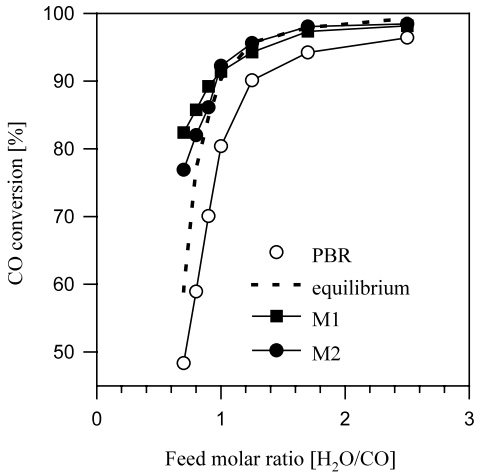

Fig. 8. Effect of molar H_2O/CO ratio on the CO conversion (feed flow 50 $cm^3\ min^{-1}$, $T = 250$ °C).

From an economical point of view, using molar ratios between 0.9 and 1.5 would be most beneficial. Xue et al. [21] claimed that a Cu–Zn catalyst was very active and selective at a molar ratio of 1.33. In addition, these findings are in good agreement with the results for dense palladium membranes reported by Basile et al. [19]. In their study, at similar experimental conditions as in this study, the CO conversion curve was observed to be above the equilibrium curve for $R < 1.5$. Basile et al. [19] found that an equimolar H_2O/CO feed molar ratio delivered the same CO conversion as the PBR with R equals two. The optimum R-value was reported to be 0.96. In this work, it was found that the use of R equals one for the PBMR gave the same CO conversion ($\approx 92\%$) as in the PBR when R was 1.6.

3.6. Comparison of the MSS-PBMR to other systems and stability aspects

MSS membranes performed well or even better in PBMR systems for the WGS reaction compared with those reported in the literature. Basile et al.

[19] showed that composite palladium membranes had a H_2 permeation of 6.25×10^{-8} mol s^{-1} m^{-2} Pa^{-1}, H_2/N_2 selectivity of 3, and a maximum CO conversion of 99.89%. They also reported a 94% conversion of CO for $R = 1$ at 300 °C. The MSS membranes in this work had H_2/N_2 separation factors of 18 and H_2 permeances of 1.5×10^{-6} mol s^{-1} m^{-2} Pa^{-1}. Under the same conditions as used by Basile et al., it was possible to achieve CO conversions of 99% for the hydrophobic membrane (M1) at a feed flow of 50 cm^3 min^{-1} and a H_2O/CO molar ratio of one. These results suggest that the MSS membranes performed slightly better than the Pd-composite membranes.

In the literature, various comparisons of porous inorganic membranes and dense membranes have been carried out [19,22,23] albeit all porous membranes had pore diameters in the region of 4 nm. According to Yildirim et al. [23], high hydrogen permselectivity is a key factor in the reactor performance. This key factor can not be met by mesoporous membranes which have much lower permselectivities for H_2/CO_2 and H_2/N_2 as activated transport is non-existent. The comparable performance of the MSS membranes makes them a good alternative to palladium membranes. They are especially suitable for the WGS reaction as the hydrogen permeance of palladium membrane decreases when the feed contains CO [24].

The overall PBMR system performed well as shown above. The ternary $Cu/Zn/Al_2O_3$ catalyst used in this experiment was selective towards the WGS reaction as no CH_4, which might be formed in side reactions, was observed in the permeate or retentate streams. Reliable operation was possible with neither membrane blockage nor catalyst deactivation observed during a full week of experiments. In addition, thermal gravimetric analysis experiments proved that no carbon was formed during the reactor operation.

4. Conclusions

A novel PBMR system with hydrophobic MSS membranes was successfully demonstrated to be suitable for the WGS reaction. Hydrophilic membranes structural changes caused by water vapour resulted in significant and unwanted changes in the permeation regimes suggesting broadening of the PSD. By the same token, hydrophobic membranes underwent slight pore closure resulting in small decrease of H_2 and CO_2 permeation while permselectivity for these gases was very similar for the conditions before and after use in the PBMR.

The good permeance characteristics of the MSS membranes and the stability of the ternary Cu-based catalyst allowed high CO conversions in the WGS reaction. PBMRs with hydrophobic membranes achieved CO conversions well above the equilibrium value for sweep gas flow rates above 20 cm^3 min^{-1}. Temperature parametric studies showed that peak CO conversion of 99% was achieved at 280 °C. The use of sweep gas shifts the reaction equilibrium to the product side enhancing CO conversion. This optimal operation was attained with a hydrophobic membrane, a sweep gas flow of 80 cm^3 min^{-1}, a feed flow rate of 50 cm^3 min^{-1} and a H_2O/CO molar ratio of 1.0.

Acknowledgements

The authors would like to acknowledge the support from the Australia Research Council (IREX and ARC Large Grants) and the Alexander von Humboldt Foundation for the Feodor-Lynen Fellowship awarded to Sabine Giessler.

References

[1] T. Utaka, K. Sekizawa, K. Eguchi, Appl. Catal. A: Gen. 194 (2000) 21.
[2] R.A. Hadden, P.J. Lambert, C. Ranson, Appl. Catal. A: Gen. 122 (1995) L1.
[3] A.J.L. Gines, N. Amadeo, M. Laborde, C.R. Apesteguia, Appl. Catal. A: Gen. 131 (1995) 283.
[4] Y. Li, Q. Fu, M. Flytzani-Stephanopoulos, Appl. Catal. B: Environ. 27 (2000) 179.
[5] S. Giessler, J.C.D. da Costa, G.Q. Lu, J. Nanosci. Nanotechnol. 1 (3) (2001) 331.
[6] R.S.A. de Lange, K. Keizer, A.J. Burggraaf, J. Membr. Sci. 104 (1995) 81.
[7] B.N. Nair, T. Yamaguchi, T. Okubo, H. Suematsu, K. Keizer, S.I. Nakao, J. Membr. Sci. 135 (1997) 237.
[8] R.M. de Vos, H. Verweij, J. Membr. Sci. 143 (1998) 37.
[9] N.K. Raman, C.J. Brinker, J. Membr. Sci. 105 (1995) 273.

[10] C. Tsai, S. Tam, Y. Lu, C.J. Brinker, J. Membr. Sci. 169 (2000) 255.
[11] R. de Vos, W.F. Maier, H. Verweij, J. Membr. Sci. 158 (1999) 277.
[12] K. Kusakabe, S. Sakamoto, T. Saie, S. Morooka, Sep. Purif. Technol. 16 (1999) 139.
[13] J.C.D. da Costa, G.Q. Lu, H.Y. Zhu, V. Rudolph, J. Porous Mater. 6 (1999) 143.
[14] J.M. van de Graaf, M. Zwiep, F. Kapteijn, J.A. Moulijn, Appl. Catal. A: Gen. 178 (1999) 225.
[15] J.C.D. da Costa, Synthesis and characterisation of molecular sieve silica (MSS) membranes, Ph.D. thesis, University of Queensland, Australia, 2000.
[16] S. Giessler, M. Duke, J.C. Diniz da Costa, G.Q. Lu, Hydrothermal stability of modified silica membranes for gas separation, 6th World Congress of Chemical Engineering, Melbourne (Australia), 23–27 September 2001 CDROM 239, 2001, pp. 1–10.
[17] K. Prabhu, S.T. Oyama, J. Membr. Sci. 176 (2000) 233.
[18] J.N. Armor, J. Membr. Sci. 147 (1998) 217.
[19] A. Basile, A. Criscuoli, F. Santella, E. Drioli, Gas Sep. Purif. 10 (1996) 243.
[20] A. Criscuoli, A. Basile, E. Drioli, Catal. Today 56 (2000) 53.
[21] E. Xue, M.O. Keeffe, J.R.H. Ross, Catal. Today 30 (1996) 107.
[22] J.S. Oklany, K. Hou, R. Hughes, Appl. Catal. A: Gen. 170 (1998) 13.
[23] Y. Yildirim, E. Gobina, R. Hughes, J. Membr. Sci. 135 (1997) 107.
[24] A. Li, W. Liang, R. Hughes, J. Membr. Sci. 165 (2000) 135.